

COMPARISON OF SEVIRI AND MODIS CLOUD PHASE DETERMINATION OVER MID-LATITUDE REGIONS

Erwin L.A. Wolters⁺, Hartwig M. Deneke^{+o}, Rob A. Roebeling⁺, and Arnout J. Feijt⁺

⁺: Royal Netherlands Meteorological Institute (KNMI), De Bilt, the Netherlands
^o: University of Bonn, Regina Pacis Weg 3, 53012 Bonn, Germany.

ABSTRACT

Cloud phase datasets obtained from the Spinning Enhanced Visible and Infra Red Imager (SEVIRI) based on the operational Climate Monitoring Satellite Application Facility (CM-SAF) algorithm are compared to cloud phase retrievals from the Moderate Resolution Imaging Spectroradiometer (MODIS). For an area of $\sim 1000 \times 1000$ km, water and ice cloud occurrence frequencies from the two algorithms for the period June-August 2006 are similar to within 5% when only overcast cloud cases are investigated. For all cloud cases (overcast + broken), differences between the CM-SAF and MODIS methods remain constant for water clouds, while for ice clouds the CM-SAF method shows a larger occurrence frequency ($\sim 11\%$) than MODIS. This is probably related to the larger pixel size of SEVIRI, which tends to underestimate the $0.6 \mu\text{m}$ and $1.6 \mu\text{m}$ channel reflectance for broken clouds. The ten-day averaged water and ice cloud occurrence frequencies over a sea and land area (both being $\sim 140 \times 140$ km) show a good correlation with $r=0.86$ and $r=0.83$ for sea and land, respectively. However, over the sea the ice cloud occurrence is permanently overestimated by the CM-SAF method.

INTRODUCTION

The thermodynamic phase of cloud particles is an important parameter for quantifying the interaction of clouds with, and affects the Earth's radiation budget differently for ice and water clouds. Therefore accurate cloud phase retrieval is of key importance. During the last few decades, several approaches to infer cloud phase from satellite imagery have been developed. When focusing on methods using only visible and near-infrared channel reflectance, most methods utilize the difference in absorption efficiency between water and ice cloud particles at the absorbing wavelengths (like e.g. the $1.6 \mu\text{m}$ and $2.1 \mu\text{m}$ spectral channels). Hansen and Pollack (1970) used the differences between visible and near-infrared reflectances to derive cloud particle phase and size. Pilewskie and Twomey (1987) performed ground-based reflectance measurements between 0.63 and $1.9 \mu\text{m}$ to derive cloud phase at convective cloud edges. Knap et al. (2002) developed a method using 1.64 - and 1.70 - μm reflectances from the Airborne Visible and Infrared Imaging Spectrometer (AVIRIS) to generate accurate cloud phase retrievals over ocean surfaces.

Although most cloud phase retrieval methods show good quality for individual cases, very few attempts have been made to evaluate the accuracy of cloud phase retrievals over longer periods, using long-term datasets. Wolters et al. (2007) showed that over mid-latitude climate regions, cloud phase derived from visible/near-infrared reflectance is better suitable to determine cloud phase climatologies (annual variation) when evaluated against ground-based derived cloud phase from lidar and cloud radar.

This paper presents first results of a comparison between a MODIS cloud phase determination method and the CM-SAF cloud phase determination method for the period June – August 2006. The focus of the research is on the water and ice cloud occurrence frequencies over longer time periods.

METHODS

a. CM-SAF cloud phase retrieval algorithm

The Satellite Facility on Climate Monitoring (CM-SAF, Woick et al., 2002) was established by the European Organization for the Exploration of Meteorological Satellites (EUMETSAT) in 2000 and is one of several SAFs set up to exploit the potential of current and future European meteorological satellites. The aim of the CM-SAF is to provide the climate research community with high quality long-term datasets for the monitoring of the climate system. Within the framework of the CM-SAF, the Royal Netherlands Meteorological Institute (KNMI) provides the algorithm for the retrieval of cloud physical properties (CPP, Jolivet and Feijt, 2005; Roebeling et al. 2006), comprising cloud optical thickness, cloud liquid water path, and cloud phase.

The cloud phase retrieval algorithm investigated here uses the 0.6 μm and 1.6 μm channel reflectance and the brightness temperature at 10.8 μm . The determination whether a SEVIRI pixel is cloudy is based on the MODIS cloud detection algorithm (Platnick et al., 2003). This algorithm has been simplified and modified to make it applicable for SEVIRI (<http://www-loa.univ-lille1.fr/~riedi/>). The input to the SEVIRI cloud detection algorithm consists of normalized reflectances from the visible (0.6 μm and 0.8 μm) and near-infrared (1.6 μm) channels, whereas brightness temperatures are used from the thermal infrared channels (3.8, 8.7, 10.8 and 12.0 μm). In addition, the algorithm uses ancillary data on solar and viewing geometry and a land/sea map.

For cloud flagged pixels, the observed 0.6 μm and 1.6 μm reflectances are compared to pre-calculated Lookup Table (LUT) reflectances from the Doubling Adding KNMI (DAK, De Haan, 1987; Stammes, 2001) radiative transfer model (RTM). The physical basis for the cloud phase retrieval is that ice crystals absorb solar radiation more effectively than water droplets at 1.6 μm and hence have a lower reflectance. The calculations are performed for spherical water droplets with an effective radius (r_{eff}) of 1-24 μm and four types of imperfect hexagonal ice crystals from the Cirrus Optical Properties ice crystal library (COP, Hess and Wiegner, 1994) with volume equivalent r_{eff} of 5, 12, 26, and 51 μm . The water and ice phase are assigned to cloud flagged pixels for which the measured 0.6 μm and 1.6 μm reflectance corresponds to the pre-calculated LUT reflectances of the respective phase. Cloud flagged pixels labeled as 'ice' with 10.8 μm -cloud top temperatures > 265 K are labeled as 'water', since for optically thin water clouds the 1.6 μm reflectance may be low enough to falsely indicate ice clouds.

b. MODIS cloud phase retrieval algorithm

The MODIS cloud phase dataset investigated here is part of the MODIS cloud product MOD06_L2 and named Cloud_Phase_Optical_Properties (Platnick et al. (2003), see <http://modis.gsfc.nasa.gov/> for more information on the data). It is one of three datasets included providing cloud phase information, and determines which phase is assumed on the optical thickness/effective radius retrieval. The method used to generate this dataset comprises several tests based on both solar and thermal radiances to indicate cloud phase. The other two MODIS cloud phase retrieval methods are named Cloud_phase_infrared and SWIR phase and utilize thermal infrared and shortwave infrared spectral radiances.

The algorithm uses cloud mask test (1.38- μm reflectance, BT3.7-BT11 and BT6.7) to initially indicate whether a cloud flagged pixel is water or ice. If from these tests an uncertain phase classification is yielded, the MODIS IR cloud phase retrieval is used instead. Finally, two additional tests are used to check the initial result. The first additional test applies the ratio of 1.6- and/or 2.1- μm reflectance to 0.67- μm reflectance, with high ratios indicating water clouds and low ratios indicating ice clouds. The second additional test uses the cloud-top temperature; cloudy pixels with a temperature < 233 K are set to ice, while pixels with temperatures > 273 K are labeled as water clouds. Platnick et al. (2003) provides a more detailed description of the separate tests used. The product is provided at 1x1 km nadir resolution.

c. MODIS-SEVIRI comparison

The CM-SAF and MODIS cloud phase were compared as follows. For a three months period (June – August 2006), all MODIS Aqua and Terra Collection 5 images were collected for an area over Western Europe (47°N-55°N, 2.5°W-8°E). In order to avoid a substantial contribution of MODIS swath edges,

the MODIS swaths should at least cover 50% of the area investigated. All MODIS 1x1 km pixels were re-projected to the SEVIRI geostationary satellite view projection. Depending on viewing geometry, 10-30 MODIS pixels were aggregated within a SEVIRI pixel. For each SEVIRI pixel, the cloud cover was obtained from the ratio of cloud flagged MODIS pixels to the total number of MODIS pixels within the SEVIRI pixel. A cloudy SEVIRI pixel was labeled overcast if > 95% of the aggregated MODIS pixels within the SEVIRI pixel were cloud flagged. Water and ice were assigned to the aggregated MODIS cloud phase retrievals if at least 95% of the cloud flagged MODIS pixels in a SEVIRI pixel were of the respective phase. If neither condition was met, the aggregated MODIS on SEVIRI cloud phase was labeled mixed phase.

For each MODIS Aqua or Terra overpass, the SEVIRI image closest in time was included in the dataset. Since SEVIRI data is available at 15-minute resolution, MODIS and SEVIRI images could be synchronized to a maximum difference of 7.5 minutes.

The water and ice cloud occurrence frequency, which is defined as the ratio of water or ice clouds to the total number of clouds for June – August 2006 within each SEVIRI pixel, were calculated for the MODIS and SEVIRI cloud phase retrievals. An analogous procedure was applied for the 10-day ice cloud occurrence frequency calculation over the 140x140 km land and sea area (see Figure 4a for their position).

RESULTS

Figure 1 shows difference plots between MODIS and SEVIRI based liquid water (left panel) and ice cloud occurrence frequency (right panel) for overcast cloud scenes only (MODIS based cloud cover > 95 %). For both phases, the largest differences occur over land. This might be linked to the more heterogeneous surface characteristics (forest, crop land, etc.) over land than over sea. In particular for thin clouds, both the MODIS and CM-SAF cloud phase determination methods are sensitive to the underlying surface. Since both methods use different spectral channel information, this sensitivity will likely be different.

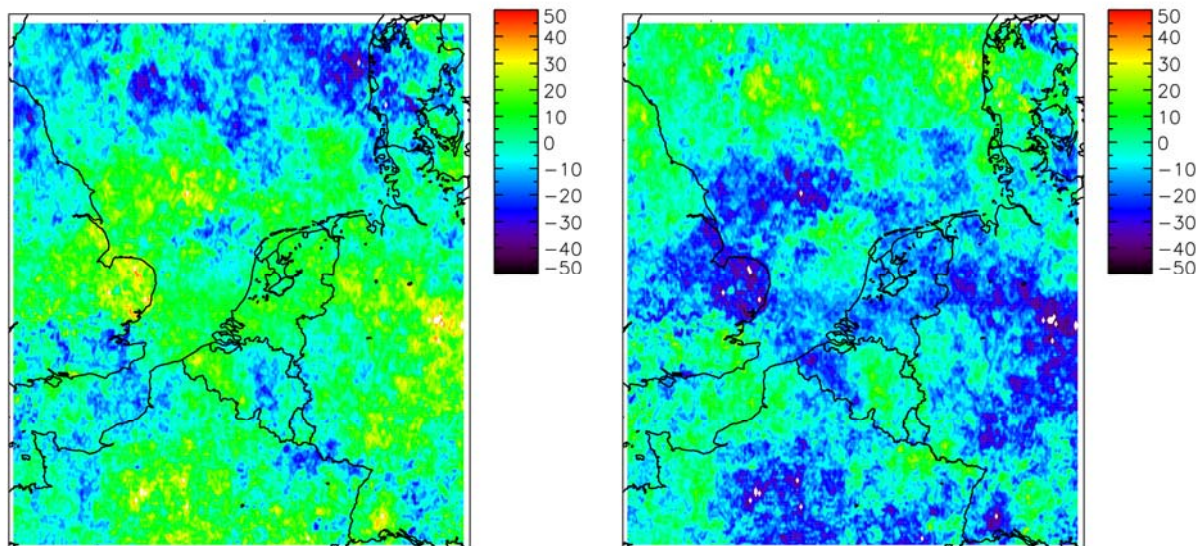


Figure 1: Difference (MODIS-SEVIRI) in retrieved liquid water (left panel) and ice cloud occurrence frequency (right panel) for overcast cloud cases in the period June – August 2006.

Figure 2 presents the histograms of differences MODIS-SEVIRI corresponding to the results shown in Figure 1. The CM-SAF algorithm retrieves slightly more (4.5%) ice clouds than the MODIS method, with the opposite for the water cloud occurrence (4.2%). The differences between water and ice cloud

occurrences do not add up to unity, due to mixed phase clouds detected by the MODIS method. The standard deviation is 14.3%, which implies that ~66% of the differences are within the range -10-19% and -19-10% for the water and ice cloud occurrence frequency differences, respectively.

When broken cloud fields are included in the dataset (Figure 3) it can be seen that there is virtually no change in the water cloud occurrence, however, the ice cloud occurrence frequency difference shifts towards a larger ice cloud overestimation by SEVIRI compared to MODIS (going from -4.5% to -11.1% difference). It is suggested that this increased difference is due to the coarse SEVIRI pixel resolution (~4x7 km at 50° N) compared to MODIS.

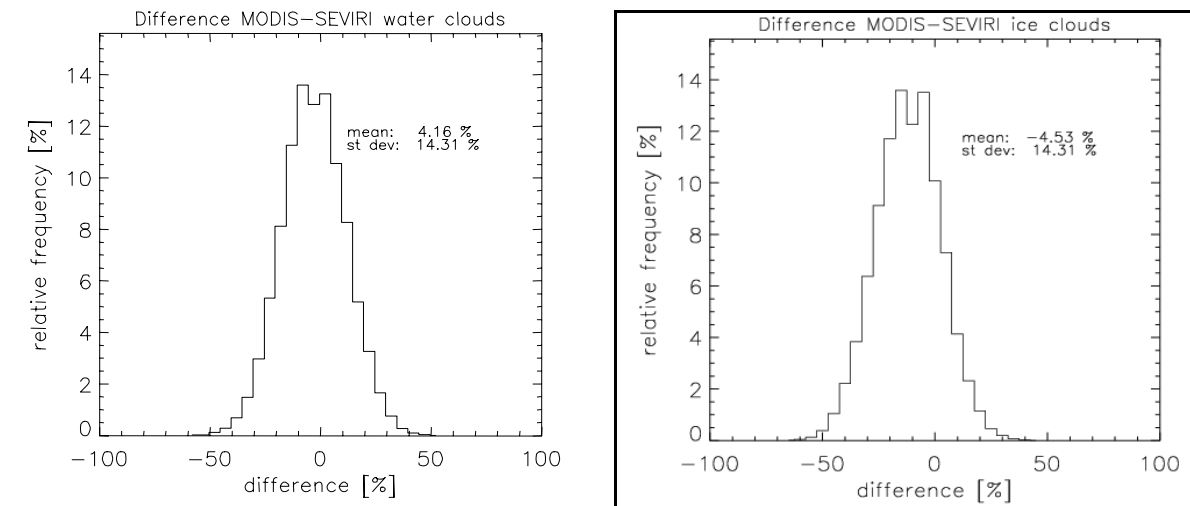


Figure 2: Frequency distributions of differences (MODIS-SEVIRI) in liquid water (left panel) and ice cloud occurrence frequency (right panel).

Broken cloud fields are hardly resolved at the SEVIRI pixel resolution of 7x4 km, while these are mostly resolved at the 1x1 km scale of the MODIS pixels. As a result, the SEVIRI 0.6 μm and 1.6 μm reflectance of the cloudy pixel will be underestimated versus the completely overcast situation, thereby increasing the probability of ice being retrieved when broken water clouds are present in reality. Further research needs to be done to assess the effect of broken cloud fields when different cloud cover thresholds are chosen.

In Figure 4, the ten-day SEVIRI (dashed lines) and MODIS (solid lines) ice cloud occurrence frequencies obtained over a sea and land area are shown (the location of the areas is shown in the left panel). The areas comprise 700 SEVIRI pixels (~14000 MODIS pixels) and only MODIS and SEVIRI images with > 20% cloud cover inside the area were included in the dataset.

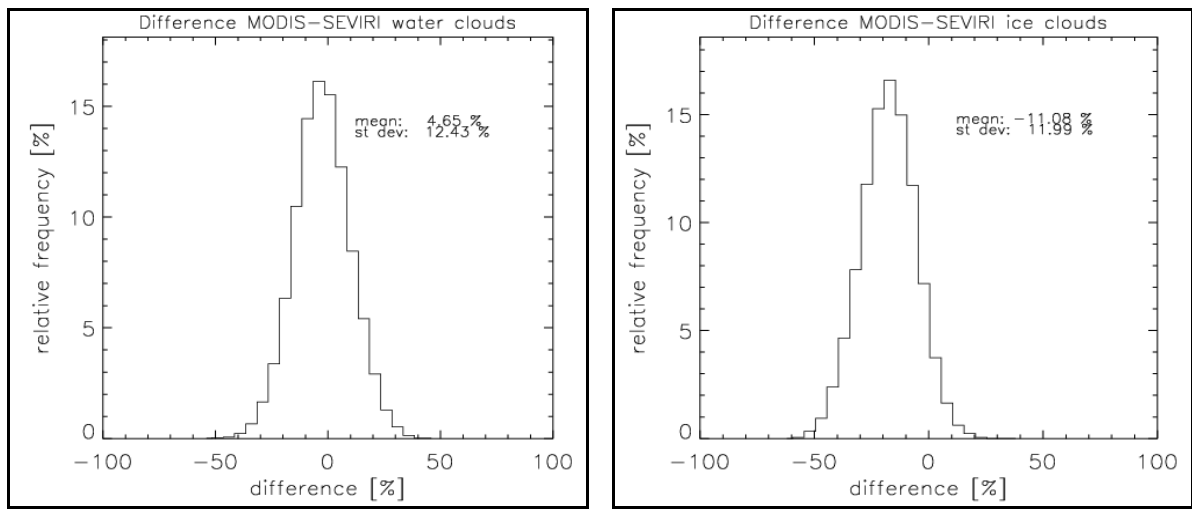


Figure 3: As Figure 2, but for all cloud cases (overcast + broken).

Overall, for both the sea and land area the derived temporal changes in the ice cloud percentage of SEVIRI and MODIS show a good correlation, with $r=0.86$ and $r=0.83$ for the sea and land area, respectively. However, it can be seen that over the sea area the CM-SAF method permanently retrieves more ice clouds (with a mean absolute difference of 15%) than the MODIS method. Over land, differences are smaller (mean absolute difference 11%). The permanent overestimation of the ice cloud percentage from SEVIRI compared to MODIS might be connected to the larger SEVIRI viewing angles in the sea area compared to over the land area ($\theta \sim 63^\circ$ versus $\theta \sim 56^\circ$). As a result, the atmospheric path length over the sea area is increased by 23% relative to the land area, which leads to more absorption by cloud particles. Moreover, at these very large viewing angles the pre-calculated lookup table reflectances become less representative.

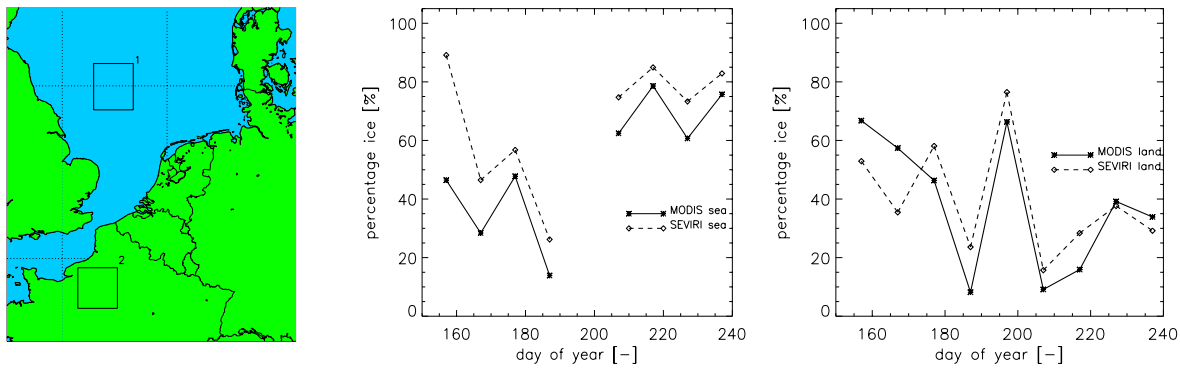


Figure 4: Map of W-Europe with the two sub-areas over sea (1) and over land (2) (left panel), ten-day averaged ice cloud occurrence frequency from MODIS (dashed) and SEVIRI (solid) over sea (middle panel) and land surface (right panel). Data points are plotted on the center day of the ten-day period.

SUMMARY AND OUTLOOK

This paper presents first results of a comparison of cloud phase datasets obtained from SEVIRI and retrieved by the operational CM-SAF algorithm, and obtained from MODIS and based on the cloud phase retrieval method which is used for the cloud optical properties retrievals. For an area of $\sim 1000 \times 1000$ km, water and ice cloud occurrence frequencies from the two algorithms for the period June-August 2006 are similar to within 5% when only overcast cloud cases are investigated.

For all cloud cases (overcast + broken), differences between the CM-SAF and MODIS methods remain approximately constant for water clouds, while for ice clouds the CM-SAF method shows a larger occurrence frequency ($\sim 11\%$) than MODIS. This is probably related to the larger pixel size of

SEVIRI, which tends to underestimate the 0.6 μm and 1.6 μm channel reflectance for broken clouds. The ten-day averaged water and ice cloud occurrence frequencies over a sea and land area show similar time signatures, with correlation coefficients of 0.86 and 0.83 for sea and land, respectively. However, over the sea area, the CM-SAF method permanently overestimates the ice cloud occurrence.

Since the two algorithms investigated in this research use different spectral tests, differences are expected to arise from both resolution effects and algorithm differences. Therefore, a comparison of cloud phase obtained from the CM-SAF method applied to both MODIS and SEVIRI data over Europe will be performed to separate the algorithm and resolution effects on the long-term water and ice cloud distribution. Especially the sensitivity to broken cloud fields will be subject of further research.

Table 1: Frequency of occurrence [in %] for cloudiness and thermodynamic phase for SEVIRI pixels calculated by aggregating collocated MODIS pixels (15x15 pixel land/sea region Netherlands, Jun-Aug. 2006).

Cloud type	Land	Sea	Cloud phase	Land	sea
Clear sky	45.1	53.8			
Broken	13.5	12.6	water	82.0	80.3
			ice	2.1	2.1
			mixed	15.9	17.6
overcast	41.4	33.6	water	54.2	59.9
			ice	26.3	23.4
			mixed	19.5	16.7

REFERENCES

De Haan, J.F., P.B. Bosma, and J.W. Hovenier, (1987), The adding method for multiple scattering calculations of polarized light, *Astron. Astroph.*, **183**, 371-391.

Hansen, J.E. and J.B. Pollack, (1970), Near-Infrared light scattering by terrestrial clouds, *Journ. Atmos. Sci.*, **27**, 265-281.

Hess, M., and M. Wiegner, (1994), COP: a data library of optical properties of hexagonal ice crystals. *Appl. Opt.*, **33**, 7740-7746.

Jolivet, D. and Feijt, A.J., (2005), Quantification of the accuracy of LWP fields derived from NOAA - 16 Advanced Very High Resolution Radiometer over three ground stations using microwave radiometers. *J. Geophys. Res.*, **110**, D11204, 10.1029/2004JD005205.

Knap, W.H., P. Stammes, and R.B.A. Koelemeijer, (2002), Cloud thermodynamic phase determination from near-infrared spectra of reflected sunlight, *Journ. Atmos. Sci.*, **59**, 83-96.

Pilewskie, P., and S. Twomey, (1987), Discrimination of ice from water clouds by optical remote sensing, *Atmos. Res.*, **21**, 113-122.

Platnick, S.E., M.D. King, S.A. Ackerman, W.P. Menzel, B.A. Baum, J.C. Riédi, and R.A. Frey, (2003), The MODIS cloud products: Algorithms and examples from Terra, *IEEE Transact. Geosc. Remote Sens.*, **41**, 459-473.

Roebeling, R.A., A.J. Feijt, and P. Stammes, (2006), Cloud property retrievals for climate monitoring: Implications of differences between Spinning Enhanced Visible and Infrared Imager (SEVIRI) on Meteosat-8 and Advanced Very High Resolution Radiometer (AVHRR) on NOAA-17. *J. Geophys. Res.*, **111**, D20210, 10.1029/2005JD006990.

Stammes, P., (2001), Spectral radiance modeling in the UV-Visible range, IRS 2000: Current problems in Atmospheric Radiation, W. L. Smith and Y. M. Timofeyev, eds., A. Deepak, Hampton, VA, 385–388.

Woick, H., Dewitte, S., Feijt, A., Gratzki, A., Hechler, P., Hollmann, R., Karlsson, K.-G., Laine, V., Löwe, P., Nitsche, H., Werscheck, M., and Wollenweber, G. (2002), The Satellite Application Facility on Climate Monitoring, *Adv. Space Res.*, 30, 2405-2410.

Wolters, E.L.A., R.A. Roebeling, and A.J. Feijt, (2007), Evaluation of cloud phase retrieval methods for SEVIRI onboard Meteosat-8 using ground-based lidar and cloud radar data. *Submitted to Journ. Appl. Meteor. Clim.*